Proc. of the European Safety and Reliability Conference (ESREL 2026)
Edited by José C. Matos, Paulo B. Lourenço, Michael Beer, Daniel Oliveira,
Edoardo Patelli, Hélder S. Sousa, Rui A. Silva and Monica Santamaria
 Published by Research Publishing, Singapore.
doi: 10.3850/ESREL2026061419_esrel26-p28996-cd

Coupling Risk Assessment Framework of Interdependent Urban Lifeline System

Yiping Bai

School of Safety Science, Tsinghua University, China. E-mail: baiyiping@tsinghua.edu.cn

Li Zhang*

School of Emergency Management and Safety Engineering, China University of Mining & Technology-Beijing, China. E-mail: BQT2510101004@student.cumtb.edu.cn

Abstract: The urban lifeline system is a complex and fragile network containing multiple interdependent subsystems, like transportation, gas, and electricity. A dynamic and quantitative model for coupling risks that balances accuracy and efficiency is both a theoretical and practical challenge. Regarding the accident evolution and control optimization of multiple lifeline systems, a systematic QRA framework comprising risk identification, risk analysis, and risk control optimization is proposed by taking energy out of control as the primary units of incidents. Multi-dimensional energy out of control is quantified by analytical and graph-based methods. Based on the emerging modelling framework, the proposed framework enables dynamic simulation of cascading failures caused by various internal and external events in lifeline systems. In the case of an LPG tank truck leakage, the spatial and temporal evolution of coupling risks in a transportation-gas-electricity system is quantified and verified, including chemical leak, explosion, power outage, gas outage, and road disruption. The critical points from spatial and functional perspectives in the lifeline system are identified and corresponding risk control suggestions for different urban areas are proposed to achieve detailed risk decoupling in the giant urban lifeline system, considering physical mechanisms. Moreover, the dominant effect of function dependency and amplification effect of spatial adjacency of coupling events in the urban lifeline system are identified.

Keywords: QRA; urban lifeline system; coupling risk; energy out of control; power grid

1. Introduction

Urban lifeline systems, including power grids, gas networks, and transportation infrastructures, serve as the blood vessel of modern cities, where subsystems are spatially intertwined and functionally interdependent. The resilience of these systems is paramount, as a localized disturbance-such as a hazardous chemical explosion-can trigger cross-system cascading failures through hidden transmission paths (Wang et al. 2026). Current urban lifelines are characterized by high-dimensional features involving human, machine, environment, and management with three-dimensional transmission (Li, 2025). The initial failure, triggered by the Wenling Liquefied Petroleum Gas (LPG) tanker explosion, results in immediate physical destruction of power grid nodes and edges within a specific blast radius (Jiang, 2023). This primary disruption, when propagated through power flow redistribution and line overloads, can trigger a domino effect that paralyzes gas, power grid, and transportation systems, posing severe threats to societal functioning and public safety.

However, traditional risk assessment methods often rely on static topology, failing to capture the dynamic physical laws of energy transport and the real-time redistribution of loads. Most existing models lack effective embedding of physical constraints such as energy transfer, transformation, and dissipation, which limits the authenticity of the simulated fault propagation process. To bridge this gap, this paper proposes a physics-driven risk quantification framework that integrates DC Power Flow (DCPF) simulation with energy out of control theory (Muhammad et al. 2025). By integrating the DCPF equations with three-dimensional energy out of control models, the framework can precisely simulate the physical threshold of the power grid - such as line overloads and voltage fluctuations - and their subsequent impact on "energy-dependent" lifeline nodes (He et al. 2024). The proposed approach enables a dynamic simulation of cascading failures from initial physical damage

to wide-area functional degradation, providing a scientific basis for decoupling strategies and proactive urban risk management.

2. Methodology

This paper proposes a quantitative risk assessment model for urban lifeline systems based on the theory of energy out of control, integrating three core modules: risk identification, coupling risk assessment, and risk control optimization, shown as Fig.1. The framework first utilizes Preliminary Hazard Analysis (PHA) to identify energy out of control forms and quantify transition points for infrastructure, generating a cross-system risk inventory. In the assessment phase, the model executes infrastructure network modelling by integrating DCPF simulation with 1D and 3D energy equations to simulate the dynamic cascading failure process from initial physical damage to functional degradation. Finally, project of emergency resource allocation is output based on the result of simulation.

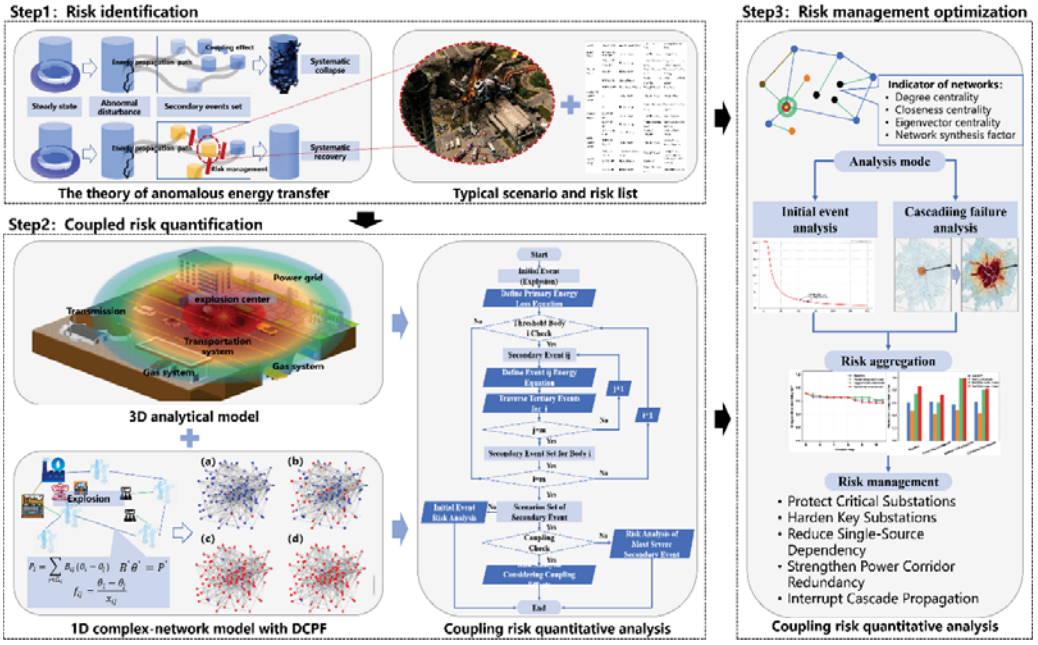

Fig. 1. Schematic diagram of the proposed quantitative risk assessment model

2.1. *Risk Identification*

Based on system theory, the urban lifeline system is represented as several interdependent subsystems, including the power, gas, and transportation networks. Incidents can be viewed as a consequence of energy out of control within infrastructure systems. The main energy forms involved in urban lifelines include kinetic, thermal, chemical, electrical, gravitational potential, and elastic potential energy. When external disturbances or internal faults disrupt normal transmission paths, these energies may affect adjacent facilities and trigger cascading consequences across subsystems.

To avoid exhaustively enumerating all possible combinations, this study organizes risk identification into a compact event ontology with four elements: energy type, initial event, secondary energy transfer, and resulting incidents. Typical initial events include leakage, impact, fire, explosion, corrosion, electric spark, and rainstorm. For instance, LPG leakage may evolve from chemical energy release into thermal and overpressure effects, causing fire, explosion, and infrastructure damage; similarly, rainstorm hazards may lead to flooding and electrical failure, further disrupting substations, roads, and dependent facilities. This abstraction forms the basis for the

subsequent coupling risk quantification. In the present case, the dominant propagation chain is identified as chemical energy release → vapor cloud explosion → localized infrastructure damage → power-flow redistribution and interdependent cascading failure.

2.2. *Coupling risk quantification*

To quantify coupling accident propagation in urban lifeline systems, a hybrid framework integrating a 1D complex-network model and a 3D analytical consequence model is developed. The 3D model is used to estimate the direct physical impact, while the 1D model is used to simulate the subsequent cascading propagation of functional failures through interdependent networks.

2.2.1. *3-Dimensional analytical model*

For accidents involving spatially distributed hazardous release, such as LPG leakage, gas leakage, and vapor cloud explosion, a three-dimensional analytical model is employed to achieve efficient consequence calculation. For high-pressure liquid release and high-pressure gas release, the released mass is estimated as

$$M_l = Q_l t = C_d \frac{A}{C_1} \cdot \sqrt{2\rho(P_0 - P_a)}t \quad (1)$$

$$M_g = Q_0 t = 1000 C A_L P_0 \sqrt{\frac{Mk}{RT}\left(\frac{2}{k+1}\right)^{\frac{k+1}{k-1}}}\, t \quad (2)$$

where Q_l and Q_0 are the liquid and gas leakage rates; C_d , C_1 , and C are discharge-related coefficients; A and A_L are the leakage areas; ρ is the liquid density; P_0 and P_a are the initial and atmospheric pressures; t is the leakage duration; M is the gas molar mass; k is the adiabatic index; R is the universal gas constant; and T is the gas temperature. The leaked gas is assumed to form a premixed cloud, whose diffusion range is estimated using either cylindrical or hemispherical spreading, depending on the release scenario.

For vapor cloud explosion, the TNO Multi-Energy method is adopted. The dimensionless overpressure is then written as

$$P' = \begin{cases} 0.2, & d' \le 0.5 \\ -0.163d' + 0.282, & 0.5 < d' \le 1 \\ 0.118{d'}^{-0.996}, & 1 < d' \le 100 \\ 0.001, & d' > 100 \end{cases} \quad (3)$$

By comparing the calculated overpressure or release consequence with the tipping point of each exposed facility, the model determines whether secondary damage and subsequent coupling failures are triggered.

2.2.2. *1-Dimensional network model with DCPF*

For one-dimensional failures propagating along lifeline networks, such as power-line outage, road blockage, and pipeline interruption, the power, gas, and transportation systems are abstracted as interdependent subnetworksA^s.

$$A^s = \begin{bmatrix} A^P & \Gamma^{PG} & \Gamma^{PR} \\ \Gamma^{GP} & A^G & \Gamma^{GR} \\ \Gamma^{RP} & \Gamma^{RG} & A^R \end{bmatrix} \quad (4)$$

where A^P , A^G , and A^R denote the intra-layer adjacency matrices of the power, gas, and road subsystems, respectively, and Γ denotes the inter-layer dependency matrix describing cross-system energy-support relations such as electricity-to-gas and electricity-to-transport coupling. After the initial physical damage caused by the explosion, cascading propagation is mainly simulated through power-flow redistribution in the power layer and electricity-support interruption in the dependent gas and transportation layers.

To update the post-disturbance state of the power subsystem, a DC power flow (DCPF) model is solved at each cascade step. For each connected component, the nodal active-power balance is expressed as

$$P_i = \sum_{j \in \Omega_i} B_{ij}(\theta_i - \theta_j) \quad (5)$$

where P_i is the net active power injection at node i, θ_i is the voltage phase angle, Ω_i is the set of nodes connected to node i, and $B_{ij} = 1/x_{ij}$is the branch susceptance.

The active power flow on branch i -j is calculated by

$$F_{ij=}B_{ij}(\theta_i - \theta_j) \quad (6)$$

When the branch flow exceeds its admissible transmission capacity, the branch is regarded as overloaded and removed in the subsequent cascade step. If the available generation within a connected component is insufficient to satisfy the total demand, load shedding is introduced before the next iteration:

$$\sum_{i\in L_k} P_i > \sum_{j\in S_k} P_j \quad (7)$$

where L_k and S_k denote the load-node set and source-node set in connected component k, respectively.

After the electric state update, the model further checks whether gas and transportation nodes still receive electricity support from nearby substations. Once the assigned supporting substation is de-energized, the corresponding dependent node is regarded as functionally failed. In this way, Two major propagation mechanisms in urban lifeline systems is identified based on the proposed model: overload-induced tripping in the power network and cross-system outage caused by loss of electricity support.

2.3. *Risk control optimization*

In this study, node importance is characterized by three classical network indicators, namely degree centrality, betweenness centrality, and eigenvector centrality.

To assess management effectiveness under DCPF-based cascading failure, network connectivity is defined dynamically rather than purely topologically. Let G_t^s denote the functional connected component of subsystem s at cascade step t, and N_0^s the initial node number. The integrated system connectivity is

$$\Phi_t^{\mathrm{sys}} = \sum_s w_s \frac{G_t^s}{N_0^s} \quad (8)$$

where w_s is the weight of subsystem s. Under DC cascading failure, connectivity degradation results not only from topological removal, but also from branch overload tripping, de-energization, and cross-system support interruption.

3. Case Study

The research object of this paper is the infrastructure system of City H, which mainly includes the city's primary road network, power transmission and distribution network, and gas network (10517 nodes and 11797 edges). Due to confidentiality requirements, some adjustments have been made to the actual layout. The layout of the city's infrastructure system at the urban scale is shown in Fig.2. To demonstrate the proposed framework, the "6.13" Wenling LPG tanker explosion is selected as the representative trigger scenario in the case study. The case is used to analyse how localized thermo-mechanical damage to substation infrastructure can initiate cascading failure and develop from discrete initial outages into wide-area contingencies through power-flow redistribution.

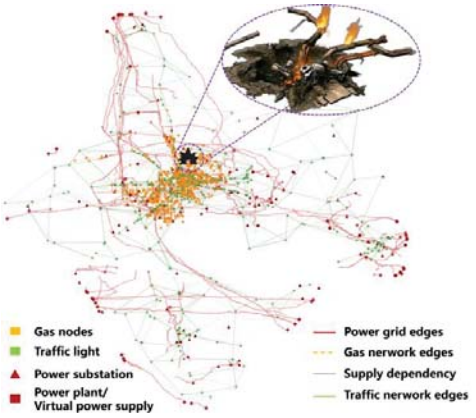

Fig. 2. Infrastructure layout and initial event locations

3.1. Assessment of the consequences of explosion

For the Wenling "6.13" LPG tanker explosion scenario, the initial out-of-control consequence was evaluated using the analytical framework introduced in Section 2.2.1. The leakage mass of pressurized LPG and the subsequent vapor-cloud explosion consequence were calculated according to the corresponding equations presented in Section 2.2.1, and the intermediate derivation is omitted here. The main input parameters of the accident scenario are summarized in Table 1.

Table 1. Main parameters of the LPG tanker explosion scenario

Parameter	Value
Tank pressure	1200 kPa
Tank volume	61.9 m³
Filling mass	25.36 t
LPG composition	60% propane & 40% butane

Leakage type	Small-hole leakage

The calculation results indicate that the released cloud could expand rapidly toward nearby infrastructures under the studied urban road environment. In this case, the flammable cloud reached a radius of about 50 m approximately 15.78 s after leakage onset, making contact with nearby potential ignition sources possible. Based on the consequence model in Section 2.2.1, the resulting explosion overpressure was then used to determine the directly damaged nodes and edges, which served as the initial trigger for the cascading-failure simulation.

3.2. Assessment of cascading failure

Following the explosion consequence analysis in Section 3.1, the cascading-failure process of the coupling power–gas–transportation network is further assessed using the DCPF-based interdependent model. The explosion first produced localized physical damage to substations and nearby links, and the disturbance then propagated through two coupling mechanisms: overload-induced tripping in the power layer and functional outage in gas and transportation infrastructures caused by the loss of electric support.

As illustrated in Fig.3, the simulation results indicate that the explosion directly damaged 10 nodes and 235 edges within the blast-affected area at step 0. Correspondingly, the served electric load immediately decreased from 13,588 MW to 11,092 MW, implying an initial load loss of 2,496 MW. This shows that the direct blast impact alone is sufficient to weaken the supply capability of the local power system and place the remaining network under stressed operating conditions.

From step 1 to step 6, the cascade propagated progressively. Already at step 1, 26 new tripped branches, 44 failed nodes, and 86 failed functional edges appeared, indicating a rapid transfer of the initial shock from the damaged power core to dependent infrastructures. During this period, the served load declined from 10,795 MW to 8,908 MW, and the number of energized substations decreased from 42 to 29, reflecting the gradual disconnection of adjacent gas and transportation facilities due to local overloads and loss of service support. A major escalation occurred at step 7, when 67 new node outages and 318 new failed functional edges were recorded, far exceeding the increases in previous steps; meanwhile, the served load dropped sharply to 7,836 MW and the number of energized substations fell to 24. This indicates a large-scale loss of supply relations between the power system and dependent gas and transportation components. After step 7, the cascade continued with a lower marginal growth rate, and the system gradually approached a degraded steady state. In the final state, the served load was reduced to 7,106 MW, with a total lost load of 6,482 MW, equivalent to 47.70% of the baseline demand.

In cumulative terms, the cascade resulted in 106 tripped power branches, 156 failed nodes, and 583 functionally failed edges, while the number of energized substations declined from 42 to 20. These results demonstrate that a localized explosion can evolve into a wide-area coupling outage once the power layer loses sufficient redundancy and can no longer maintain service to dependent infrastructures.

To further examine the effectiveness of different risk control interventions under the same explosion-triggered disturbance, three strategies (power-edge reinforcement, support-link redundancy, and combined intervention) are compared. (Shown as Table2).

Table 2. Risk control strategies and corresponding parameter adjustments

Strategies	Parameter adjustment description
Power-edge reinforcement	Increasing the transmission capacity $F_{ij}^{\max}$ of key power edges associated with high-importance nodes identified in 2.3.
Support-link redundancy	Enlarging the equivalent support-substation set by increasing the support-search parameters
Combined intervention	Simultaneously adjusting both the power-edge capacity and the support-link redundancy parameters

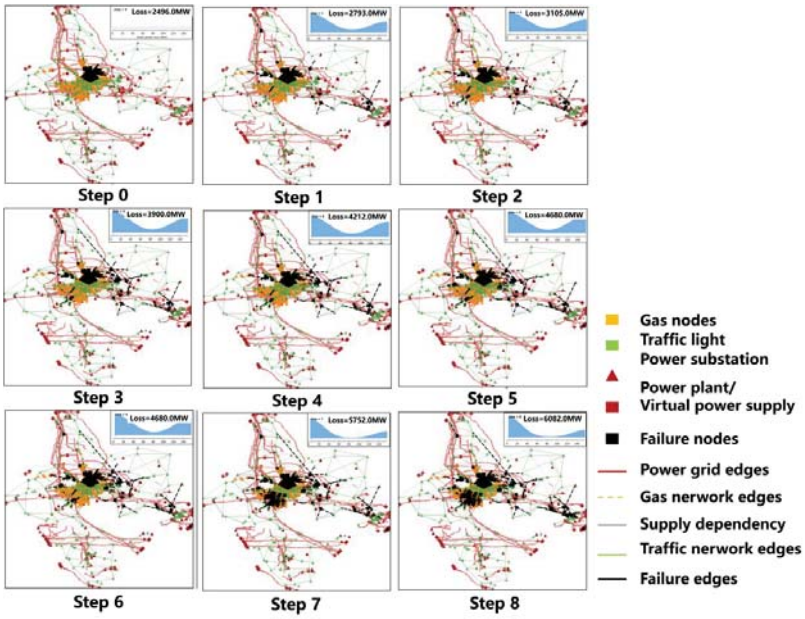

Fig. 3. Infrastructure layout and initial event locations

According to Eqs. (19) and (20), the intervention performance is evaluated in terms of integrated connectivity preservation and cascade-scale suppression. As shown in Fig.4 and Fig.5, the connectivity evolution, all three strategies mitigate the post-disturbance functional degradation to some extent; however, their effects differ in the later stages of the cascade. Power-edge reinforcement maintains the highest integrated connectivity overall, while support-link redundancy provides only limited improvement. The combined intervention does not show a significant advantage over power-edge reinforcement in connectivity preservation, indicating that the marginal benefit of adding support-link redundancy is relatively small in the present scenario.

Among the three risk control strategies, power-edge reinforcement achieves the best overall performance, yielding the lowest final lost-load ratio and the smallest numbers of failed nodes and failed edges. In contrast, support-link redundancy performs worst in terms of cascade containment, with larger final disruption levels across multiple indicators. The combined intervention slightly improves some failure metrics compared with support-link redundancy, but its overall benefit remains close to that of power-edge reinforcement rather than showing a clear synergistic gain. The spatial evolution of failures provides additional evidence for the dominant role of power-network reinforcement. Under power-edge reinforcement, the failure spread remains more concentrated around the initially affected area, and the outward propagation along major transmission corridors is more effectively constrained. By contrast, support-link redundancy cannot substantially alter the main propagation pattern, suggesting that the cascade is still governed primarily by overload redistribution and de-energization within the power subsystem. Therefore, under the present DCPF-based cascading-failure scenario, reinforcing critical power edges is more effective than merely increasing interdependent support redundancy.

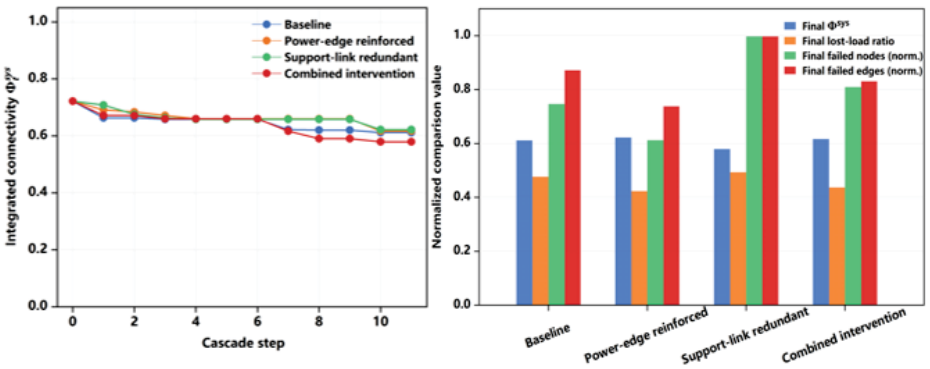

Fig. 4. Connectivity preservation under different risk control strategies (left), Final cascading scale and connectivity comparison (right)

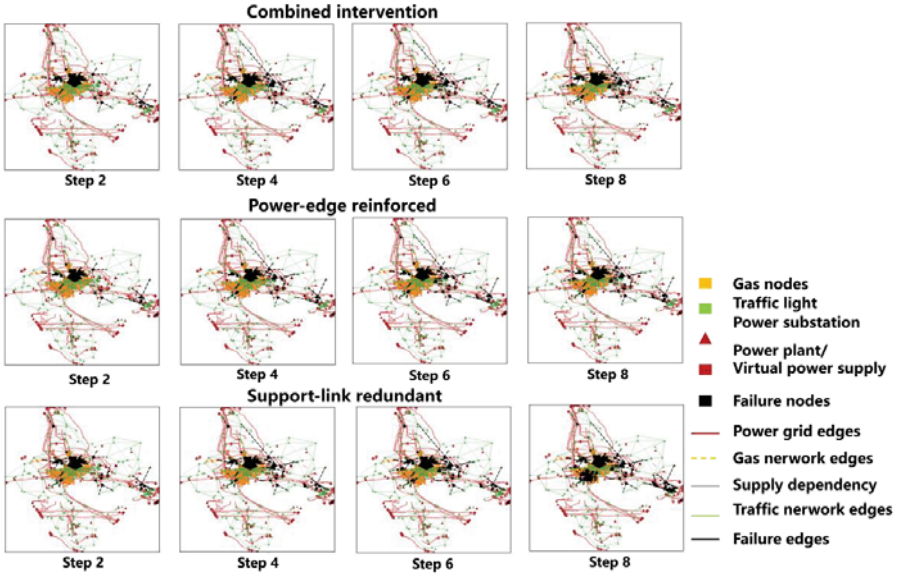

Fig. 5. Infrastructure layout and initial event locations

4. Discussions

The results indicate that the coupling urban lifeline system exhibits a power-dominated cascading pattern under the studied explosion scenario. Although the initial event is an LPG explosion, the subsequent large-scale disruption is governed mainly by power-flow redistribution, branch overloading, and progressive de-energization in the power subsystem. As electric support declines, dependent gas and transportation nodes rapidly lose functionality, accelerating the degradation of the overall coupling system. This suggests that, in interdependent urban infrastructures, the dominant cascade channel may differ from the initial disturbance source and plays a more critical role in risk assessment.

The comparison of risk control strategies further supports this mechanism. Power-edge reinforcement performs better than support-link redundancy in preserving connectivity and suppressing the final cascade, while the combined strategy provides only limited additional benefit. This implies that resilience improvement in the present case depends mainly on strengthening

critical transmission corridors and enhancing the carrying capacity of key power edges. From a practical perspective, mitigation efforts should therefore prioritize critical substations and major transmission corridors in dense urban areas. It should also be noted that the present framework is based on DCPF and simplified interdependency assumptions, making it more suitable for comparative evaluation of intervention effectiveness than for exact prediction of all post-disaster operating states.

5. Conclusions

A quantitative risk assessment framework for urban lifeline systems is developed by integrating energy out of control theory, multi-dimensional consequence model, and a DCPF-based interdependent network model. Key findings reveal that:

The case study shows that the LPG tanker explosion initially damaged 10 nodes and 235 edges, reducing the served electric load from 13,588 MW to 11,092 MW. The disturbance then propagated through overload tripping, de-energization, and cross-system dependency loss, and finally reduced the served load to 7,106 MW, corresponding to a total load loss of 6,482 MW, which accounts for 47% of the baseline demand.

The power subsystem is the dominant propagation medium in the coupling power–gas–transportation network. The abrupt escalation in the later cascade stage suggests the existence of a functional tipping point, beyond which outage propagation expands rapidly and amplifies the final system consequence far beyond the directly damaged area.

The comparison of risk control strategies shows that power-edge reinforcement is more effective than support-link redundancy in preserving system connectivity and suppressing cascade expansion. Therefore, protecting critical substations and reinforcing major power corridors should be regarded as the primary strategy for cascade mitigation and resilience enhancement.

Acknowledgement

This work is supported by the National Key Research and Development Program of China (Grant No. 2023YFC3807602), the National Natural Science Foundation of China (Grant No. 72504159, 72442008).

References

Wang, J., & Huang, Y. (2026). An edge load cascading failure model and vulnerability analysis of coupled critical infrastructure networks: Considering functional and geographical interdependency. In Reliability Engineering and System Safety. 266, 111719-111719.

Yu, F., Fan, B., Li, X. Y., et al. (2020). Improving emergency preparedness to cascading disasters: A case-driven risk ontology modelling. In Journal of Contingencies and Crisis Management. 28(3), 194-214.

Mora, L., Gerli, P., Ardito, L., et al. (2023). Smart city governance from an innovation management perspective: Theoretical framing, review of current practices, and future research agenda. In Technovation 123, 102717.

Li, P., Cheng, Y., Zhang, Y., et al. (2025). Cascading failure tolerance of manufacturing services collaboration network toward industrial internet platforms. In The International Journal of Advanced Manufacturing Technology. 136(11), 1-19.

Ma, Z., Hu, D., Chien, S., et al. (2025). Robustness of Urban Rail Transit Networks Considering Cascade Failure under Attacks: A Case Study of Nanjing, China. ASCE-ASME Journal of Risk and Uncertainty in Engineering Systems, Part A: Civil Engineering. 11(1).

Xie, Q., Liu, X., & Wu, S. (2025). Resilience-based optimisation framework for post-earthquake restoration of power systems. Reliability Engineering & System Safety, 257, 110808.

Jiang, X., Chen, J., Chen, M., et al. (2020). Multi-stage dynamic post-disaster recovery strategy for distribution networks considering integrated energy and transportation networks. Journal of Power and Energy Systems, 7(2), 408-420.

Muhammad Qasim Khan, Muhammad Mansoor Khan, Arshad Nawaz, et al. A Vector Control-based Design of Multi-port Interline DC Power Flow Controller for HVDC System. Electric Power Systems Research. 248, 111766.

He, S.Z., Zhou, Y.X., Zhou, Y.D., et al. (2024). Data-Driven Identification Model of Vulnerable Set for Cascading Failure in Power Grid. IEEE Transactions on Automation Science and Engineering. 22, 3097-3112